Technetium-99m-Tetrofosmin to Assess Myocardial Blood Flow: Experimental Validation in an Intact Canine Model of Ischemia

Albert J. Sinusas, QingXin Shi, Mitchell T. Saltzberg, Peter Vitols, Diwakar Jain, Frans J. Th. Wackers and Barry L. Zaret

Experimental Nuclear Cardiology Laboratory, Division of Cardiovascular Medicine, Department of Internal Medicine, at Yale University, School of Medicine, New Haven, Connecticut

Technetium-99m-tetrofosmin is a ^{99m}Tc-labeled perfusion tracer demonstrating promise for myocardial perfusion imaging. To determine if ^{99m}Tc-tetrofosmin tracks myocardial flow over a pathophysiologic range, the initial myocardial uptake and clearance of ^{99m}Tc-tetrofosmin relative to microsphere flow were evaluated in a canine model of ischemia during pharmacological vasodilatation. **Methods:** Six open-chest dogs were subjected to complete left anterior descending coronary artery occlusion. Dogs were injected with ^{99m}Tc-tetrofosmin and radiolabeled microspheres during pharmacological stress. Coincident with radiotracer injection, dynamic planar imaging and arterial sampling were performed to assess ^{99m}Tc-tetrofosmin clearance from blood, myocardium, lung and liver. Fifteen minutes after injection, hearts were excised for well counting of myocardial ^{99m}Tc-tetrofosmin activity and flow. **Results:** Myocardial ^{99m}Tc-tetrofosmin activity correlated linearly with microsphere flow ($r = 0.84$). Relative ^{99m}Tc-tetrofosmin activity underestimated flow at higher flow ranges (>2.0 ml/min/g) and overestimated flow in low flow ranges (<0.2 ml/min/g). Technetium-99m-tetrofosmin cleared rapidly from the blood and was retained in the myocardium. Resting target-to-background activity ratios (heart:lung = 3.57 ± 1.01; heart:liver = 0.58 ± 0.04) were acceptable 10 min after injection. **Conclusion:** Our experimental data support both the validity of ^{99m}Tc-tetrofosmin as a myocardial perfusion tracer and the use of early poststress ^{99m}Tc-tetrofosmin imaging for the assessment of myocardial perfusion in man.

Key Words: technetium-99m-tetrofosmin; myocardial perfusion imaging

J Nucl Med 1994; 35:664–671

Technetium-99m is a preferred radionuclide for clinical gamma camera imaging because of favorable physical properties, ease of production and relatively low cost. Major efforts have been directed at development of a ^{99m}Tc-labeled myocardial perfusion tracer. Initial development involved cationic ^{99m}Tc complexes (*1,2*). Although preliminary animal experiments were promising (*3*), these agents demonstrated unfavorable heart-to-background activity ratios in humans (*4,5*). Efforts were then directed at two different classes of compounds: cationic isonitrile ^{99m}Tc (I) complexes (*6–11*), and neutral, lipophilic, ^{99m}Tc complexes (boronic acid adducts of technetium dioxime (BATO) complexes) (*12–15*). One agent in each of these classes has recently been approved for clinical imaging: ^{99m}Tc-sestamibi and ^{99m}Tc-teboroxime.

Additional efforts have been directed recently at the development of a new class of ^{99m}Tc-labeled lipophilic cations, which employ a diphosphine ligand (*16–19*). Two ^{99m}Tc-labeled phosphines have undergone preliminary testing in patients and show promise for clinical myocardial perfusion imaging (*17,20,21*). One of these diphosphine compounds, 1,2-bis[bis(2-ethoxyethyl) phosphino] ethane (^{99m}Tc-tetrofosmin) can be rapidly prepared from a freeze-dried kit formulation (*19*).

The purpose of this study was to determine if ^{99m}Tc-tetrofosmin is a reliable myocardial flow tracer over a pathophysiologic range of flows encountered in ischemia and infarction. The initial myocardial uptake and clearance characteristics of ^{99m}Tc-tetrofosmin relative to microsphere flow were evaluated in a canine model of ischemia during pharmacological vasodilatation.

METHODS

Surgical Preparation

Experiments were performed in fasting adult mongrel dogs (mean weight, 20.3 ± 2.7 kg, range 18.2–21.8 kg), anesthetized with intravenous sodium thiamylal (20 mg/kg). Animals were intubated and mechanically ventilated on a respirator with halothane (0.5%–2%), nitrous oxide and oxygen ($N_2O:O_2$ = 3:1). A single electrocardiographic lead was monitored continuously. One femoral vein and both femoral arteries were isolated and cannulated for administration of fluids, drugs and ^{99m}Tc-tetrofosmin,

Received Apr. 8, 1993; revision accepted Aug. 12, 1993.

For correspondence or reprints contact: Albert J. Sinusas, MD, Nuclear Cardiology, Yale University School of Medicine, PO Box 3333, 333 Cedar St., TE-2, New Haven, CT 06510.

pressure monitoring and arterial sampling. Arterial pH, partial pressure of carbon dioxide (PCO_2) and partial pressure of oxygen (PO_2) were measured serially, and the ventilator adjusted to maintain these parameters within the physiologic range. A balloon flotation catheter was placed in the pulmonary artery for measurement of central temperature and cardiac output.

A thoracotomy was performed in the fifth intercostal space and the heart suspended in a pericardial cradle. A flared polyethylene catheter was placed in the left atrium for the injection of radiolabeled microspheres. The proximal left anterior descending coronary artery (LAD), after the first major diagonal branch, was isolated for placement of a hydraulic occluder (model VO-3, Rhodes Medical Instruments). A Doppler flow probe (Crystal Biotech; Hopkinton, MA) was placed on the LAD just proximal to the occluder.

All experiments were performed with approval of the Yale Animal Care and Use Committee, in compliance with the position of the American Heart Association on research animal use.

Experimental Protocols

Six dogs were subjected to complete LAD occlusion followed by pharmacological stress. Two dogs received intravenous adenosine in an incremental fashion (160 μg/kg/min and 320 μg/kg/min) over 18 min. The adenosine infusion was continued for 4 min after the intravenous injection of 30 mCi of ^{99m}Tc-tetrofosmin. Four dogs received intravenous dipyridamole over 4 min (0.12 mg/kg/min). Technetium-99m-tetrofosmin (30 mCi) was injected intravenously during peak pharmacological stress 4 min after completion of the dipyridamole infusion. Coincident with ^{99m}Tc-tetrofosmin injection, dynamic planar imaging (5 sec/frame) was performed in four dogs in the lateral projection over 15 min. Serial arterial blood samples (1 ml) were collected in five dogs every 5 sec for 5 min followed by every 15 sec for 10 min via a roller pump (Harvard Apparatus, Model 2501-001).

Radiolabeled microspheres (^{113}Sn, ^{103}Ru, ^{95}Nb, ^{46}Sc) for the measurement of regional myocardial blood flow were injected into the left atrium at baseline, coronary artery occlusion and peak pharmacological stress. For each determination, radiolabeled microspheres (2–12 million, mean diameter, 11 μm) suspended in 10% dextran and Tween-80 were injected over 15 sec, followed by a normal saline flush (5 ml). The microsphere suspension was vortexed (Vortex Genie Mixer, Evanston, IL) and hand agitated between 2–5 ml syringes immediately prior to injection in order to assure adequate mixing. Paired arterial samples were withdrawn over 95 sec beginning 5 sec before the microsphere injection for the calculation of myocardial blood flow according to the methods of Heymann et al. (*22*).

Postmortem Analysis

The hearts were rapidly excised at 15 min after injection of ^{99m}Tc-tetrofosmin and were divided from base to apex into four slices of equal thickness (1–1.5 cm thick). The slices were incubated in a buffered triphenyl tetrazolium chloride (TTC) solution for 15 min at 38°C to detect myocardial necrosis.

Determination of Regional Myocardial Blood Flow and ^{99m}Tc-Tetrofosmin Activity

Each of the myocardial slices was cut into eight radial sections, which were subdivided into epicardial, midwall, and endocardial segments, thereby resulting in a total of 96 segments per heart for quantification of myocardial ^{99m}Tc-tetrofosmin activity and blood flow. Gamma well scintillation counting to measure ^{99m}Tc-tetrofosmin activity of myocardial samples was performed at 48 hr after excision. Myocardial and arterial blood samples were counted 5 days later for the determination of regional myocardial blood flow. Separation of isotopes by energy windows (^{99m}Tc, 130–170 keV; ^{113}Sn, 340–440 keV; ^{103}Ru, 450–550 keV; ^{95}Nb, 650–840 keV; ^{46}Sc, 850–1300 keV) was performed according to the methods of Heymann et al. (*22*) with spill-down and spill-up correction.

Myocardial activity (cpm/g) was correlated with myocardial flow (ml/min/g) in each dog. To facilitate comparisons between dogs, myocardial ^{99m}Tc-tetrofosmin activity and flow were normalized by two separate methods. First, myocardial ^{99m}Tc-tetrofosmin activity and flow were expressed as a percentage of nonischemic zones using a previously reported method (*23*). The nonischemic values were computed from 15 segments from the posterolateral free wall. This method evaluates flow and activity in the ischemic region relative to a normal region in a fashion analogous to the interpretation of clinical images. Second, myocardial ^{99m}Tc-tetrofosmin activity and flow in each myocardial segment was normalized by the computed average activity or flow for each corresponding dog, as previously proposed (*24*).

Image Analysis

Technetium-99m-tetrofosmin clearance curves were derived from analysis of dynamic planar imaging sequences obtained in four of the dogs. All image analysis was performed on a Picker PCS computer. Four by four pixel regions of interest (ROIs) were placed over the central ischemic and nonischemic myocardial regions, lung and liver. The location of the central ischemic region was identified on the lateral images by placement of a ^{99m}Tc radioactive point source in the central ischemic region during acquisition of a static image. Clearance curves for myocardium, lung and liver were generated from serial images using average measured counts within the ROIs for each dog. In order to pool the results from each dog, all values were expressed as a percentage of the average nonischemic myocardial value derived from an image acquired over the minute before euthanization.

Statistical Analysis

All data are presented as the mean ± 1 s.e.m. Normality of the distribution was verified with either the Wilk-Shapiro test or the Kolmogorov-Smirnov test, depending on the population size. Univariate analysis of groups was performed by a paired Student's t-test, unpaired two sample t-test, Wilcoxon signed rank test, or Wilcoxon rank signed test (Statistical package, RS/1 Bolt, Beraneck, Newman, Cambridge, MA). Selection of the statistical test was performed automatically by the software based on the results of normality testing. Differences between groups were considered significant at $p < 0.05$ (two-tailed). Linear regression analysis was used to compare paired samples and the correlation coefficient(s) expressed.

RESULTS

A total of six dogs underwent coronary occlusion followed by pharmacological stress. None of the dogs developed ventricular fibrillation or demonstrated evidence of myocardial necrosis on postmortem histochemical staining.

Hemodynamic Measurements

Heart rate and mean systolic pressure were recorded before coronary occlusion (baseline), during coronary artery occlusion (occlusion), during peak pharmacological

TABLE 1
Myocardial Flow Measurement

	Transmural flow (ml/min/g)		
	Baseline	Occlusion	Peak stress
Ischemic	1.02 ± 0.14	0.27 ± 0.14*	0.21 ± 0.09*
Nonischemic	0.92 ± 0.11	0.97 ± 0.14	1.96 ± 0.41*

*$p \leq 0.05$ versus baseline.
Microspheres were injected before coronary occlusion (baseline), during coronary artery occlusion (occlusion) and during peak pharmacological stress (peak stress).

stress (peak stress), and at the time of euthanization (poststress). Heart rate did not change throughout the protocol (baseline: 100 ± 9; occlusion: 108 ± 10; peak stress: 101 ± 13; poststress: 114 ± 11). Systolic pressure did not change with coronary artery occlusion (baseline: 116 ± 10; occlusion: 114 ± 11). However, systolic pressure decreased significantly during pharmacological stress (peak stress: 79 ± 4, $p \leq 0.05$), although returned toward baseline at the time of euthanization (poststress: 85 ± 2).

Measurement of Myocardial Flow

Absolute microsphere flow in the central ischemic and nonischemic regions during baseline, coronary occlusion and pharmacological stress are summarized in Table 1.

Correlation of ^{99m}Tc-Tetrofosmin Activity and Regional Myocardial Blood Flow

Myocardial ^{99m}Tc-tetrofosmin activity 15 min after injection correlated linearly with microsphere flow during peak stress in each dog (Fig. 1). The correlation coefficients ranged from 0.71 to 0.94. The best correlations were seen in the two dogs injected with ^{99m}Tc-tetrofosmin during adenosine stress (Fig. 1A, B). In these dogs, peak myocardial flow did not exceed 2.0 ml/min/g. Dipyridamole stress increased flow in some dogs to greater than 4.0 ml/min/g. In each dog, the plot of ^{99m}Tc-tetrofosmin activity versus flow achieved a plateau at higher flow ranges (greater than 2.0 ml/min/g). Myocardial ^{99m}Tc-tetrofosmin activity appeared to underestimate flow at flows exceeding 1.5–2.0 ml/min/g.

In order to pool the results from all six dogs, myocardial ^{99m}Tc-tetrofosmin activity and microsphere flow in each myocardial segment (n = 576) were normalized by two approaches (Fig. 2). Among all dogs there was an excellent correlation between myocardial ^{99m}Tc-tetrofosmin activity and flow, both when values were normalized to a nonischemic region (r = 0.87) and to computed dog averages (r = 0.87). The results for adenosine (n = 2) and dipyridamole (n = 4) stress were comparable. Therefore, the results from all six dogs were pooled. The normalized plots of myocardial ^{99m}Tc-tetrofosmin activity and flow demonstrate an overestimation of flow in the low flow range and underestimation of flow in the high flow range.

Average myocardial flow and ^{99m}Tc-tetrofosmin activity in the central ischemic area were also computed (percentage of nonischemic), since interpretation of ^{99m}Tc-tetrofosmin images is based on analysis of changes in relative tracer intensity in the ischemic area (Fig. 3). Flow in the central ischemic area was 24.2% ± 8.5% nonischemic (%NI) during coronary occlusion. Relative flow in the central ischemic area decreased significantly during pharmacological stress (9.6 ± 2.1 %NI; $p < 0.05$). Technetium-99m-tetrofosmin activity in the central ischemic area (27.1 ± 6.3 %NI), 15 min after injection, underestimated the flow decrement at the time of injection ($p < 0.05$).

Blood ^{99m}Tc-Tetrofosmin Clearance

Arterial ^{99m}Tc-tetrofosmin activity was measured serially and expressed as a percentage of peak arterial activity (Fig. 4). Technetium-99m-tetrofosmin activity cleared rapidly from the blood. Blood activity at 5 and 15 min after injection was 2.8% ± 0.9% and 0.8% ± 0.3% of peak activity, respectively.

Organ ^{99m}Tc-Tetrofosmin Clearance: Assessment with Dynamic Planar Imaging

In four dogs, dynamic planar imaging was performed to evaluate the clearance of ^{99m}Tc-tetrofosmin from the heart, lung and liver (Figs. 5 and 6). Myocardial clearance of ^{99m}Tc-tetrofosmin was slow. Between 3 and 15 min postinjection the myocardial activity cleared 18% ± 11% in the ischemic region. Technetium-99m-tetrofosmin clearance was similar in both ischemic and nonischemic regions over the initial 15 min after injection. Lung activity remained lower than myocardial activity. Liver activity remained elevated over the initial 15 min postinjection. The heart-to-liver ratios at 5, 10 and 15 min after injection were calculated at 0.68 ± 0.07, 0.58 ± 0.04 and 0.60 ± 0.02, respectively.

DISCUSSION

In a canine model of ischemia, we have demonstrated that ^{99m}Tc-tetrofosmin is a reliable flow tracer over a range of flows produced during pharmacological stress. Myocardial ^{99m}Tc-tetrofosmin activity 15 min after injection correlated linearly with microsphere flow at the time of injection when flow did not exceed 2.0 ml/min/g. At higher flow ranges, relative ^{99m}Tc-tetrofosmin activity underestimated relative microsphere flow. In low flow ranges, relative myocardial ^{99m}Tc-tetrofosmin activity overestimated relative microsphere flow, thereby potentially underestimating the flow deficit. Technetium-99m-tetrofosmin cleared rapidly from the blood and was retained in the myocardium. No significant differences were observed in myocardial clearance between ischemic and nonischemic regions over the initial 15 min after injection. In this anesthetized canine preparation, liver activity remained elevated during the early postinjection period. Target-to-background activity ratios were similar to other available ^{99m}Tc-labeled myocardial perfusion tracers. Early poststress ^{99m}Tc-tetrofosmin planar gamma camera imaging was feasible and reliable for the assessment of stress-induced flow heterogeneity.

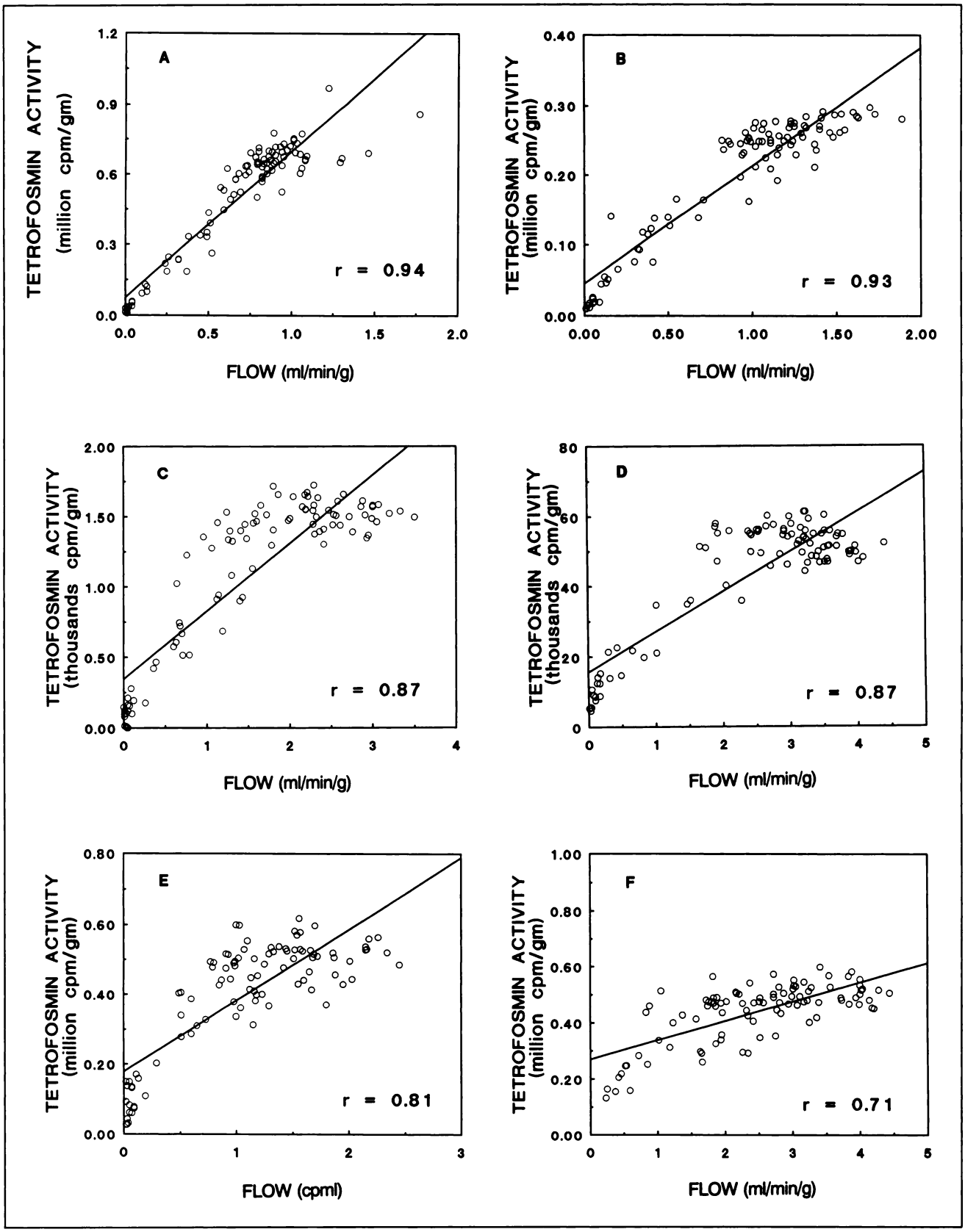

FIGURE 1. Correlation of ^{99m}Tc-tetrofosmin activity (cpm/g) and microsphere flow (ml/min/g) for each of the six dogs. Different x- and y-axis scales are used for each dog. Myocardial ^{99m}Tc-tetrofosmin activity increased linearly with flow, when flow did not exceed 2 ml/min/g.

Correlation of ^{99m}Tc-Tetrofosmin Activity and Regional Myocardial Blood Flow and Relationship to Other Tracers

Hearts were excised at 15 min after stress injection of ^{99m}Tc-tetrofosmin to determine if the early poststress myocardial distribution of ^{99m}Tc-tetrofosmin accurately reflected stress-induced flow heterogeneity. The early myocardial distribution of ^{99m}Tc-tetrofosmin activity correlated with microsphere flow during both adenosine and dipyridamole stress. Both pharmacological stress agents cause coronary vasodilation which is mediated via adenosine. Data from the dogs receiving adenosine and dipyridamole were pooled since the relationships between myocardial ^{99m}Tc-tetrofosmin activity and flow were not significantly different. Average flow in the nonischemic region increased to 1.96 ± 0.41 ml/min/g. In some dogs, myocardial flow increased to greater than 4 ml/min/g.

At higher flow ranges (greater than 2 ml/min/g) ^{99m}Tc-tetrofosmin uptake underestimated flow. A similar underestimation of flow has been observed with ^{201}Tl (*25,26*). Myocardial ^{201}Tl activity during adenosine stress may underestimate flow as a consequence of reduction in net myocardial extraction of thallium independent of flow (*27*).

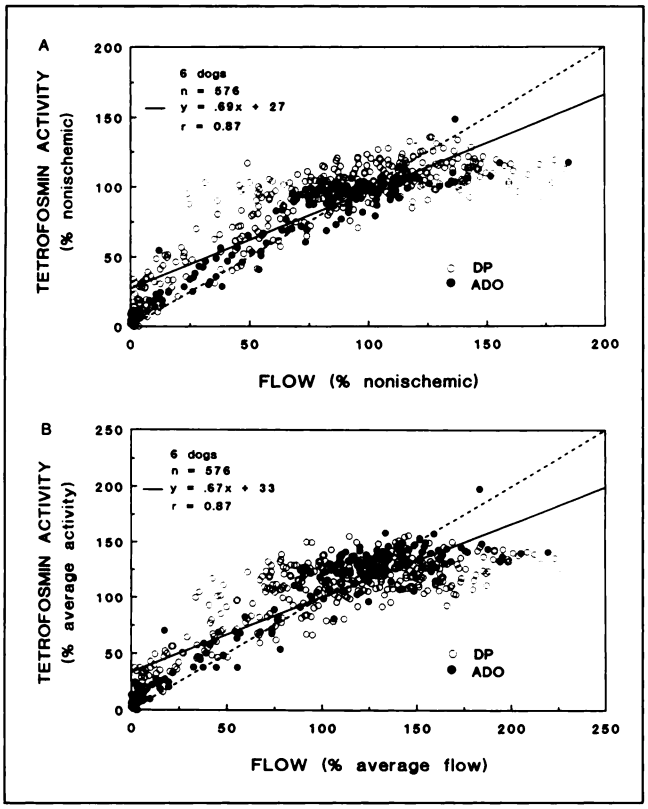

FIGURE 2. Normalized ^{99m}Tc-tetrofosmin activity and microsphere flow. Technetium-99m-tetrofosmin activity and flow were normalized to both nonischemic values (A) and mean values for each dog (B). A total of 576 segments were analyzed among six dogs. The filled circles represent segments from dogs subjected to adenosine (ADO) stress. Open circles represent data from dogs subjected to dipyridamole stress (DP). The correlations are derived from pooled data from all six dogs.

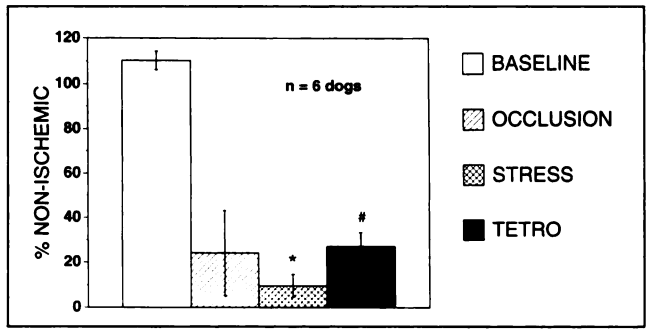

FIGURE 3. Comparison of relative flow and ^{99m}Tc-tetrofosmin (TETRO) activity in the central ischemic area (15 segments). Microsphere flow (% nonischemic) was measured before coronary artery occlusion (baseline), during left anterior descending artery occlusion (occlusion) and during peak pharmacological stress (stress). Flow in the ischemic area decreased significantly during pharmacological stress (*$p < 0.05$, stress flow versus occlusion flow). Relative ^{99m}Tc-tetrofosmin activity (% nonischemic) underestimated the relative flow deficit at 15 min after injection (#$p < 0.05$, TETRO activity versus occlusion flow).

This effect may be due to a metabolic perturbation or possibly related to alterations in perfusion pressure. Glover et al. demonstrated that during vasodilation with dipyridamole, the myocardial distribution of ^{99m}Tc-sestamibi was also linearly related to flow up to approximately 2.0 ml/min/g (*28*). However, at higher flow the myocardial activity of ^{99m}Tc-sestamibi similarly underestimated flow. Over the first 20 min after injection, the relationship of myocardial ^{201}Tl and ^{99m}Tc-sestamibi activity and flow declines (*25*). Myocardial ^{99m}Tc-teboroxime activity immediately (1 min) after injection is linearly related to flow, at flows up to 4.5 ml/min/g (*29*). However, by 5 min after injection, ^{99m}Tc-teboroxime also underestimates flow in the moderately high flow ranges.

We also demonstrated increased relative myocardial ^{99m}Tc-tetrofosmin activity in the low flow regions comparable to ^{201}Tl and ^{99m}Tc-sestamibi (*23,30–32*). The increased uptake of these diffusable radiotracers under conditions of low flow results from more efficient tissue extraction associated with longer transit times (*33*). Studies employing a blood perfused isolated rabbit heart preparation have demonstrated that myocardial extraction of ^{201}Tl, ^{99m}Tc-sestamibi and teboroxime are all inversely related to blood flow (*15,34*). Using the same blood-perfused isolated rabbit heart preparation, Dahlberg et al. recently demonstrated that the "uptake" of ^{99m}Tc-tetrofosmin increased linearly with flow (*35*). In these experiments, "uptake" was defined as the product of net extraction (Enet) and coronary flow.

Blood and Organ ^{99m}Tc-Tetrofosmin Clearance

The early evaluation of myocardial tracer distribution may be complicated by cardiac blood pool and background activity. The clinical application of ^{99m}Tc-tetrofosmin imaging potentially may be confounded by prominent hepatic activity adjacent to the heart. In our anesthetized canine preparation, hepatic activity remained elevated at 15 min

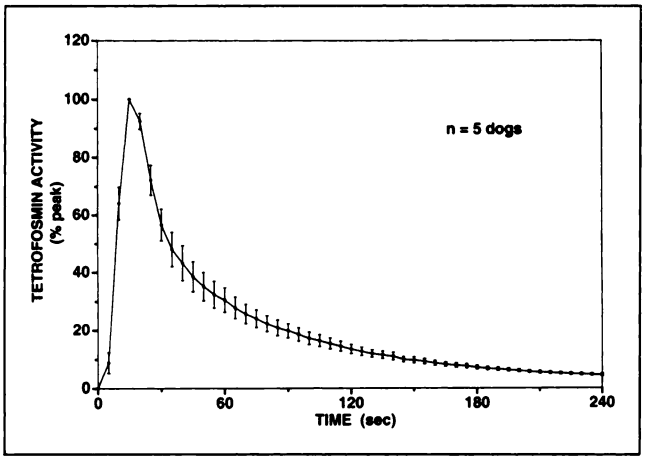

FIGURE 4. Arterial blood clearance of ^{99m}Tc-tetrofosmin. Measured ^{99m}Tc-tetrofosmin activity (n = 5 dogs) is expressed as percent peak activity (mean ± s.e.m.).

after an intravenous injection of ^{99m}Tc-tetrofosmin during pharmacological stress with both adenosine and dipyridamole. The heart-to-liver ratio at 15 min after injection was calculated at 0.6.

Initial clinical evaluation of the biodistribution ^{99m}Tc-tetrofosmin in humans suggests good myocardial retention of ^{99m}Tc-tetrofosmin in the heart and rapid background clearance, thereby permitting high quality myocardial images as early as 5 min after injection (*20,36*). Following a resting injection of ^{99m}Tc-tetrofosmin in humans, the heart-to-lung ratio of ^{99m}Tc-tetrofosmin was 3.1 ± 1.8 and 4.5 ± 1.5 at 5 and 30 min after injection, respectively. Lung clearance of ^{99m}Tc-tetrofosmin is rapid and should not interfere with early image interpretation (*20*). In contrast, the heart-to-liver ratio was 0.4 ± 0.1 and 0.6 ± 0.3, respectively, at 5 and 30 min after a resting injection. In this previously reported clinical study (*20*), the heart-to-liver ratios of ^{99m}Tc-tetrofosmin were more optimal following exercise (5 min: 0.8 ± 0.3; 30 min: 1.2 ± 0.7). Jain et al.

FIGURE 5. Dynamic lateral ^{99m}Tc-tetrofosmin imaging sequence. Static images were acquired every 5 sec. Shown are composite 1-min images acquired during the first 10 min after injection. The initial image (upper left) reflects right ventricular (superior) and left ventricular (inferior) blood-pool activity. The apex of the heart points toward the lower left corner of each image. The liver is seen below the heart. The rib spreader produces an attenuation defect in the superior aspect of the liver. A large dense anteroapical perfusion defect is seen as early as 4 min after ^{99m}Tc-tetrofosmin injection (arrow).

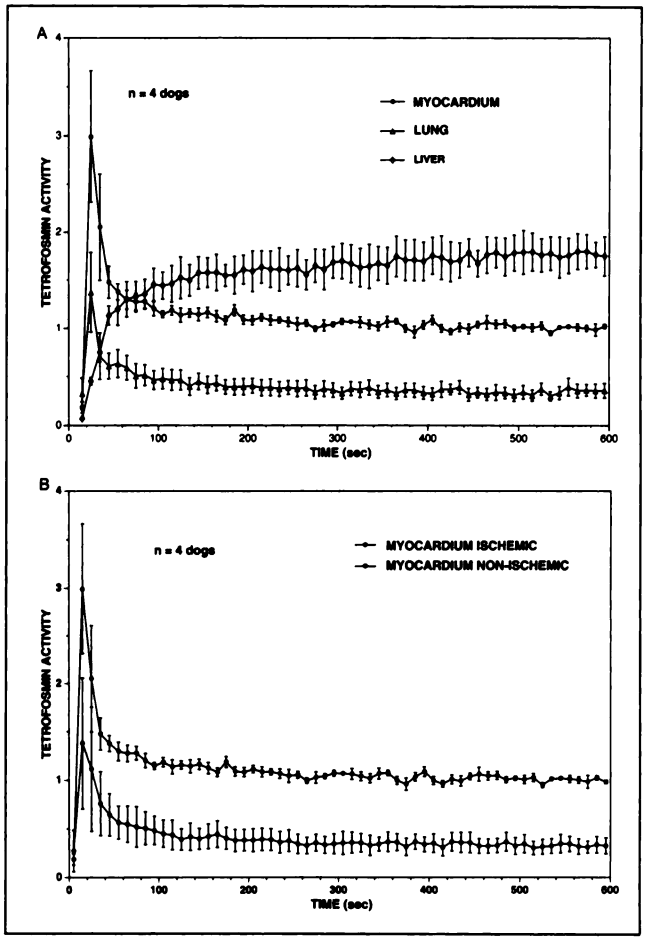

FIGURE 6. Technetium-99m-tetrofosmin tissue clearance curves. Technetium-99m-tetrofosmin activity is expressed as a percentage of the nonischemic myocardial activity at the time of euthanasia. Although images were obtained every 5 sec, the data derived from every other image in the dynamic sequence are shown for clarity. Lung activity remained lower than myocardial activity (A). Liver activity remained elevated over the initial 10 min postinjection (A). There was slow clearance from both ischemic and nonischemic regions of the heart (B, mean ± s.e.m.).

(*36*) used a same-day stress-rest protocol and observed improved heart-to-liver ratios at rest (5 min: 0.8 ± 0.2; 30 min: 1.0 ± 0.2) in comparison to the study by Higley et al. (*20*). This suggests that the impact of hepatic activity on rest image interpretation has not as yet been resolved.

Analysis of the biodistribution of ^{99m}Tc-sestamibi in man demonstrated a heart-to-liver ratio of 0.5 ± 0.1 at both 5 and 30 min after a resting injection (*11*). Following injection of ^{99m}Tc-sestamibi at peak exercise, the heart-to-liver ratios were 1.3 ± 0.1 and 1.4 ± 0.2 at 5 and 30 min after injection, respectively (*11*). Thus, hepatic clearance of ^{99m}Tc-tetrofosmin relative to the heart appears comparable to that previously reported for ^{99m}Tc-sestamibi under resting conditions.

Clinical Implications

Pharmacological stress with adenosine or dipyridamole in conjunction with ^{201}Tl (*37–42*) ^{99m}Tc-sestamibi (*43*) or ^{99m}Tc-teboroxime (*44,45*) has proved useful for the detec-

tion of coronary artery disease. For the optimal detection of pharmacologically induced ischemia, early imaging is necessary. Unfortunately, early imaging with all myocardial tracers is complicated by initial blood-pool activity and extracardiac background.

Our experimental data support the proposed use of early poststress ^{99m}Tc-tetrofosmin imaging for the assessment of myocardial perfusion in humans. A multicenter clinical study involving 218 patients suggested that exercise-rest ^{99m}Tc-tetrofosmin planar imaging was comparable diagnostically to planar exercise-redistribution ^{201}Tl scintigraphy for characterization of ischemia and scar (*21*). These investigators employed a single-day, "split dose" stress and rest protocol. Although ^{99m}Tc-tetrofosmin is predominantly cleared by the hepatobiliary system, subdiaphragmatic activity reportedly did not interfere with image interpretation in most patients. This study suggested that poststress imaging is possible as early as 15 min after injection.

Although the initial myocardial clearance of ^{99m}Tc-tetrofosmin was slow, further studies are necessary to determine if there is differential washout of ^{99m}Tc-tetrofosmin from ischemic and nonischemic regions.

ACKNOWLEDGMENTS

This research was supported in part by a Grant-in-Aid of the American Heart Association, Connecticut Affiliate. The ^{99m}Tc-tetrofosmin utilized in these experimental studies was provided by Medi-Physics, Inc., Arlington Heights, IL.

REFERENCES

1. Deutsch E, Glaven K, Sodd V, Nishiyama H, Ferguson D, Lukes S. Cationic ^{99m}Tc complexes as potential myocardial imaging agents. *J Nucl Med* 1981;22:287–907.
2. Ketring A, Troutner D, Volkert W, Holmes R. Technetium-99m complexes of lipophilic cyclam derivatives; assessment of potential myocardial imaging agents [Abstract]. *J Nucl Med* 1982;23:p17.
3. Nishiyama H, Deutsch E, Adolph R, et al. Basel kinetics studies of ^{99m}Tc DMPE as a myocardial imaging agent in the dog. *J Nucl Med* 1982;23:1093–1101.
4. Dudczak R, Angelberger P, Homan R, Kletter K, Schmoliner R, Frischauf H. Evaluation of ^{99m}Tc-dichlorobis (1-2 dimethylphosphino) ethane (^{99m}Tc-DMPE) for myocardial scintigraphy in man. *Eur J Nucl Med* 1983;8:513–515.
5. Gerundini P, Savi A, Gilardi M, et al. Evaluation in dogs and humans of three potential technetium-99m myocardial perfusion agents. *J Nucl Med* 1986;27:409–416.
6. Jones A, Abrams M, Davison A, et al. Biological studies of a new class of technetium complexes: the hexakis (alkylisonitrile technetium (I) cations. *Int J Nucl Med Biol* 1984;11:225–234.
7. Holman B, Jones A, Lister-James J, et al. A new ^{99m}Tc-labeled myocardial imaging agent hexakis (t-butyisonitrile)-[Technetium (I) ^{99m}Tc TBI]: initial experience in the human. *J Nucl Med* 1984;25:1350–1355.
8. Sia S, Holman B, McKusick K, et al. The utilization of ^{99m}Tc TBI as a myocardial perfusion agent in exercise studies: comparison with ^{201}Tl thallus chloride and examination of its biodistribution in humans. *Eur J Nucl Med* 1986;12:333–336.
9. Holman B, Campbell C, Lister-James J, Jones A, Davison A, Kloner R. Effect of reperfusion and hyperemia on the myocardial distribution of technetium-99m-t-butyisonitrile. *J Nucl Med* 1986;27:1172–1177.
10. Holman B, Sporn V, Jones A, et al. Myocardial imaging with technetium-99m CPI: initial experience in the human. *J Nucl Med* 1987;28:13–18.
11. Wackers F, Berman D, Maddahi J, et al. Technetium-99m hexakis-2-methoxyisobutyl isonitrile: human biodistribution, dosimetry, safety, and preliminary comparison to thallium-201 for myocardial perfusion imaging. *J Nucl Med* 1989;30:301–311.
12. Treher E, Gougoutas J, Malley M, et al. New technetium radiopharmaceuticals: boronic acid adducts of vicinal dioxime complexes. *J Lab Compd Radiopharm* 1986;23:118–120.
13. Maublant J, Moins N, Gachon P. Uptake and release of two new ^{99m}Tc-labeled myocardial blood flow imaging agents in cultured cardiac cells. *Eur J Nucl Med* 1989;15:180–182.
14. Narra R, Nunn A, Kucyzynski B, Feld T, Wedeking P, Eckelman W. A neutral technetium-99m complex for myocardial imaging. *J Nucl Med* 1989; 30:1830–1837.
15. Leppo J, Meerdink D. Comparative myocardial extraction of two technetium-labeled BATO derivatives (SQ30217-SQ32014) and thallium. *J Nucl Med* 1990;31:67–74.
16. Marmion M, Kwiatkowski M, Nosco D, et al. Chemistry of a new class of ^{99m}Tc myocardial perfusion agents with optimized imaging properties [Abstract]. *J Nucl Med* 1991;32:925.
17. Rossetti C, Vanoli G, Paganelli G, et al. Q12: a new ^{99m}Tc myocardial perfusion agent with optimized imaging properties: evaluation in humans [Abstract]. *J Nucl Med* 1991;32:1007.
18. Smith F, Smith T, Gemmell H, et al. Phase I study of ^{99m}Tc diphosphine (P53) for myocardial imaging [Abstract]. *J Nucl Med* 1991;32:967.
19. Kelly J, Forster A, Higley B, et al. Technetium-99m-tetrofosmin as a new radiopharmaceutical for myocardial perfusion imaging. *J Nucl Med* 1993; 34:222–227.
20. Higley B, Smith F, Gemmell H, et al. Technetium-99m-1,2-bis[bis(2-ethoxyethyl)phosphino]ethane: human biodistribution, dosimetry and safety of a new myocardial perfusion imaging agent. *J Nucl Med* 1993;34:30–38.
21. Tetrofosmin Study Group. Comparative myocardial perfusion imaging with ^{99m}Tc-tetrofosmin and thallium-201: results of phase III international trial. *Circulation* 1992;86:I-506.
22. Heymann M, Payne B, Hoffman J, Rudolph A. Blood flow measurements with radionuclide-labeled particles. *Prog Cardiovasc Dis* 1977;20:55–79.
23. Sinusas A, Watson D, Cannon J, Beller G. Effect of ischemia and postischemic dysfunction on myocardial uptake of technetium-99m-labeled methoxyisobutyl isonitrile and thallium-201. *J Am Coll Cardiol* 1989;14:1785–1793.
24. Yipintsoi T, Dobbs W, Scalon P, Knopp T, Bassingthwaighte J. Regional distribution of diffusible tracers and carbonized microspheres in the left ventricle of isolated dog hearts. *Circ Res* 1973;33:573–587.
25. Melon P, Beanlands R, DeGrado T, Nguyen N, Petry N, Schwaiger M. Comparison of technetium-99m sestamibi and thallium-201 retention characteristics in canine myocardium. *J Am Coll Cardiol* 1992;20:1277–1283.
26. Sinusas A, Daher E, Shi Q-X, et al. Arbutamine: a new pharmacological stress agent for potential use with thallium-201 scintigraphy. *J Am Coll Cardiol* 1993;21:377A.
27. Dahlberg S, Gilmore M, Leppo J. Adenosine reduces myocardial thallium-201 "uptake" in the isolated rabbit heart. *Circulation* 1992;I-706.
28. Glover D, Okada R. Myocardial kinetics of Tc-MIBI in canine myocardium after dipyridamole. *Circulation* 1990;81:628–637.
29. Beanlands R, Muzik O, Nguyen N, Petry N, Schwaiger M. The relationship between myocardial retention of technetium-99m teboroxime and myocardial blood flow. *J Am Coll Cardiol* 1992;20:712–719.
30. Strauss H, Harrison K, Langan J, Lebowitz E, Pitt B. Thallium-201 for myocardial imaging: relationship of thallium-201 to regional myocardial perfusion. *Circulation* 1975;51:641–645.
31. Pohost G, Okada R, O'Keefe D, et al. Thallium redistribution in dogs with severe coronary stenosis of fixed caliber. *Circ Res* 1981;48:439–446.
32. Li Q, Frank T, Franceschi D, Wagner H, Becker L. Technetium-99m-methoxyisbutyle isonitrile (RP-30) for quantification of myocardial ischemia and reperfusion in dogs. *J Nucl Med* 1988;29:1539–1548.
33. Sangren W, Sheppard C. A mathematical derivation of the extraction of a labeled substance between a liquid flowing in a vessel and an external compartment. *Bull Math Biophys* 1953;15:387–393.
34. Leppo J, Meerdink D. Comparison of the myocardial uptake of a technetium-labeled isonitrile analog and thallium. *Circ Res* 1989;65:632–639.
35. Dahlberg S, Gilmore M, Leppo J. Effect of coronary blood flow on the "uptake" of tetrofosmin in the isolated rabbit heart. *J Nucl Med* 1992;5:846.
36. Jain D, Wackers F, Mattera J, McMahon M, Sinusas A, Zaret B. Biokinetics of ^{99m}Tc-tetrofosmin, a new myocardial perfusion imaging agent: implications for a one-day imaging protocol. *J Nucl Med* 1993;34:1254–1259.
37. Gould K, Westcott R, Albro P, Hamilton G. Noninvasive assessment of coronary stenoses by myocardial imaging during pharmacological coronary vasodilation: II. Clinical methodology and feasibility. *Am J Cardiol* 1978; 41:279–287.
38. Ruddy T, Dighero H, Newell J, et al. Quantitative analysis of dipyridamole-

thallium images for the detection of coronary artery disease. *J Am Coll Cardiol* 1987;10:142–149.
39. Verani M, Mahmarian J, Hixson J, Boyce T, Staudacher R. Diagnosis of coronary artery disease by controlled coronary vasodilation with adenosine and thallium-201 scintigraphy in patients unable to exercise. *Circulation* 1990;82:80–87.
40. Nguyen T, Heo J, Ogilby D, Iskandrian A. Single photon emission computer tomography with thallium-201 during adenosine-induced coronary hyperemia: correlation with coronary arteriography, exercise thallium imaging and two-dimensional echocardiography. *J Am Coll Cardiol* 1990;16: 1375–1383.
41. Coyne E, Belvedere D, Vande Streek P, Weiland F, Evans R, Sparceavento L. Thallium-201 scintigraphy after intravenous infusion of adenosine compared with exercise thallium testing in the diagnosis of coronary artery disease. *J Am Coll Cardiol* 1991;17:1289–1294.
42. Gupta N, Esterbrooks D, Hilleman D, Hohiuddin S. Comparison of adenosine and exercise thallium-201 single-photon emission computed tomography (SPECT) myocardial perfusion imaging. *J Am Coll Cardiol* 1992;19: 248–257.
43. Tartagni F, Dondi M, Limonetti P, et al. Dipyridamole technetium-99m-2-methoxy isobutyl isonitrile tomoscintigraphic imaging for identifying disease coronary vessels: comparison with thallium-201 stress-rest study. *J Nucl Med* 1991;32:369–376.
44. Labonte C, Taillefer R, Lambert R, et al. Comparison between technetium-99m-teboroxime and thallium-201 dipyridamole planar myocardial perfusion imaging in detection of coronary artery disease. *Am J Cardiol* 1992;69:90–96.
45. Iskandrian A, Heo J, Nguyen T, et al. Tomographic myocardial perfusion imaging with technetium-99m teboroxime during adenosine-induced coronary hyperemia: correlation with thallium-201 imaging. *J Am Coll Cardiol* 1992;19:307–312.

(continued from page 663)

Three patients were found to have effusions of between 200 and 300 cc, and in two of these three patients the diagnostic criteria for pericardial effusion were not completely satisfied. Thus in the presence of cardiomegaly, a 200-cc effusion may not widen the x-ray silhouette enough to satisfy all the criteria for effusion which we have established.

It is apparent, therefore, that in patients with effusions of 200–300 cc, a diagnosis of pericardial effusion by radioisotope scanning will depend upon the size of the heart.

The results of this study indicated that pericardial effusions of more than 300 cc can be diagnosed accurately by radioisotope scanning, and notably in those patients without cardiomegaly, as little as 200 cc may be detected.The lateral border of the heart is never sharp for a variety of reasons: constant motion of the heart; respiration; collimator resolution. One important factor contributing to this problem is scatter from the high-energy gammas produced by I^{131} in its decay. Better cardiac scans could be attained by use of monoenergetic, lower-energy radioisotopes.

In 23 patients undergoing open-heart surgery in whom the pericardial contents were accurately measured, and in 11 additional patients examined at autopsy or by pericardiocentesis, isotopic photoscans of the heart were made and the results were correlated.

J Nucl Med 1965;5:101-111

Condensed from *15 Years Ago:*

"Circumferential Profiles:" A New Method for Computer Analysis of Thallium-201 Myocardial Perfusion Images

Robert D. Burow, Malcolm Pond, A. William Schafer and Lewis Becker

The Johns Hopkins University School of Medicine, Baltimore, Maryland

A method for computer analysis of thallium-201 scintigrams is described, in which the left ventricular activity is measured along radii constructed from the center of the left ventricle (LV) to each point on the LV circumference. Data are then displayed graphically as a "circumferential profile" of normalized activity against radial location. Thallium defects are identified and scored by comparison of the profile curve with empirically determined normal limits. In patients with coronary artery disease, defect scores were found to be quantitative and reproducible, and to agree generally with subjective visual analysis.

J Nucl Med 1979; 20:771-777